FEBS Letters 589 (2015) 871–879

FEBS Letters

journal homepage: www.FEBSLetters.org

The role of *Drosophila* TNF Eiger in developmental and damage-induced neuronal apoptosis

Jeny Shklover, Flonia Levy-Adam, Estee Kurant *

Department of Genetics and Developmental Biology, The Rappaport Family Institute for Research in the Medical Sciences, Faculty of Medicine, Technion – Israel Institute of Technology, Haifa 31096, Israel

ARTICLE INFO

Article history:
Received 1 October 2014
Revised 17 February 2015
Accepted 27 February 2015
Available online 6 March 2015

Edited by Ned Mantei

Keywords:
Apoptosis
CNS
Drosophila
Eiger
Embryo
hid

ABSTRACT

Eiger, the sole *Drosophila* TNF-alpha homolog, causes ectopic apoptosis through JNK pathway activation. Yet, its role in developmental apoptosis remains unclear. *eiger* mutant flies are viable and fertile but display compromised elimination of oncogenic cells and extracellular bacteria. Here we show that Eiger, specifically expressed in embryonic neurons and glia, is not involved in developmental neuronal apoptosis or in apoptotic cell clearance. Instead, we provide evidence that Eiger is required for damage-induced apoptosis in the embryonic CNS through regulation of the pro-apoptotic gene *hid* independently of the JNK pathway. Our study thus reveals a new requirement for Eiger in eliminating damaged cells during development.

© 2015 The Authors. Published by Elsevier B.V. on behalf of the Federation of European Biochemical Societies. This is an open access article under the CC BY-NC-ND license (http://creativecommons.org/licenses/by-nc-nd/4.0/).

1. Introduction

The tumor necrosis factor (TNF) superfamily contains type II transmembrane/secreted proteins that play a crucial role in different physiological processes such as cell proliferation, differentiation, immunity and apoptosis [1–3]. In vertebrates, TNF is involved in the innate inflammatory response as well as in the transition from innate to acquired immunity [4,5]. The molecular mechanisms underlying TNF function in different processes, specifically in apoptosis, are not well understood [6,7]. To address this issue we use the *Drosophila* model, in which there is no inflammatory reaction or adaptive immunity and therefore cell death is uncoupled from inflammation.

The *Drosophila* genome encodes a single TNF homolog, *eiger*, which like many of its mammalian counterparts induces cell death through c-Jun N-terminal kinase (JNK) pathway activation in the eye and wing [8,9]. *eiger* mutant flies show no obvious morphological defects, but have reduced resistance to extracellular pathogens [10]. Additionally, Eiger is involved in the regulation of the pro-apoptotic gene *head involution defective (hid)* in primordial germ cells [11], in crystal cell rupture after larval injury [12], in fate determination during neuroblast division [13] and in induction of glial cell division following developmental programmed cell death (PCD) and injury in the adult brain [14]. Eiger has been reported to act as a tumor suppressor in the elimination of oncogenic epithelial cells [15] or as a pro-tumor factor [16].

Despite the fact that Eiger was initially discovered through its pro-apoptotic ability, little is known about its role in apoptosis during development (developmental apoptosis). Here, we test Eiger's role during embryogenesis, in neuronal apoptosis and glial phagocytosis of apoptotic neurons. We show that Eiger is specifically expressed in certain neurons and glia of the embryonic CNS. Using loss-of-function and gain-of-function approaches, we demonstrate that Eiger is not involved in developmental apoptosis or glial phagocytosis of apoptotic neurons. Rather, we uncover a novel role for Eiger in ionizing radiation (IR)-damage-induced apoptosis through regulation of expression of the pro-apoptotic gene *hid* and in neuronal apoptosis, which we stimulate by overexpressing *hid* in embryonic neurons. We furthermore provide evidence that, in the absence of *eiger*, developing neurons are refractory to HID-induced apoptosis. These data demonstrate that Eiger is required for elimination of damaged neurons during development.

Authors contributions: J.S. and F. L.-A. performed the experiments, J.S., F. L.-A. and E.K. interpreted the data, E.K. wrote the manuscript.

* Corresponding author at: Department of Genetics and Developmental Biology, Rappaport Faculty of Medicine, Technion, Efron Street, P.O. Box 9697, Haifa 31096, Israel. Fax: +972 4 8295403.

E-mail address: kurante@tx.technion.ac.il (E. Kurant).

http://dx.doi.org/10.1016/j.febslet.2015.02.032
0014-5793/© 2015 The Authors. Published by Elsevier B.V. on behalf of the Federation of European Biochemical Societies.
This is an open access article under the CC BY-NC-ND license (http://creativecommons.org/licenses/by-nc-nd/4.0/).

2. Materials and methods

2.1. Fly strains

The following fly strains were used in this work: *repoGal4* (B. Jones), *UAScytGFP* (# 1521; Bloomington), *UAShid* (E. Arama), *Df (3L) H99* (H. Steller), *simu-cytGFP* and *simu* [17], *UASnucGFP* (# 4775; Bloomington), *elavGal4* (O. Schuldiner), *eigerGal4* (G.W. Davis), *UASeiger* (M. Miura), *puclacZ = puc[E69]* (A. Salzberg), *TRE-eGFP* (D. Bohmann). All strains were raised at 25 °C. *w1118* flies were used as wild type control.

2.2. Immunohistochemistry and live imaging

For immunohistochemistry embryos were fixed and stained according to standard procedures. Primary antibodies were used at following dilutions: guinea pig anti-SIMU [18] at 1:2500, rabbit anti-activated caspase 3 (CM1, BD) and mouse anti-GFP (Roche) at 1:50 and 1:100, respectively, mouse anti-REPO and rat anti-ELAV (Hybridoma bank) at 1:5 and 1:100, respectively, rabbit anti-Eiger (M. Miura) was preabsorbed and used at 1:250, mouse anti-DAC at 1:5, anti-EVE at 1:100 and anti-CUT at 1:50 (Hybridoma bank), anti-TH (Millipore) at 1:100. Fluorescent secondary antibodies (Cy3/Jackson ImmunoResearch; Alexa Fluor 488/Molecular Probes) were used at 1:200 dilutions. All confocal images were acquired on a confocal microscope Zeiss LSM 700 using a Plan-Apochromat 20×/0.8 M27 lens. 80% Glycerol solution was used as the imaging medium. Image analysis was performed using Zeiss LSM 700 and Imaris (Bitplane) software. Live imaging was carried out by dechorionating embryos, mounting them under Halocarbon oil, injecting 2–3% egg volume LysoTracker (Molecular Probes) as described in [19]. *In situ* hybridization was performed using standard procedures.

2.3. Western blot analysis

Embryo extracts were prepared in lysis buffer containing 50 mM Tris–HCl, pH 7.4, 150 mM NaCl, 1 mM EDTA, 0.5% Triton X-100, supplemented with a mixture of protease inhibitors (Roche), using a hand homogenizer. Protein concentration was determined (Bradford reagent, Bio-Rad), and 100 μg protein was used for SDS–PAGE. After electrophoresis, proteins were transferred to a PVDF membrane (Bio-Rad) and probed with a rabbit anti-HID (Santa Cruz) antibody followed by HRP-conjugated secondary antibody (Jackson ImmunoResearch) and an enhanced chemiluminescent substrate (Bio-rad).

2.4. qRT-PCR

RNA was isolated from embryos using RNazol®RT (MRC). Following DNase treatment RNA was used as a template for cDNA synthesis (M-MLVRT and RNasin: Promega). Gene expression was evaluated using TaqMan gene expression assays (Applied Biosystems) specific for *hid* (Dm01823029_m1) and RpL32 (Dm02151827 as an internal control). The PCR reactions were set up following the manufacturer's instructions. The assays were performed in triplicate with RNA samples from at least three different isolations. Relative gene expression was quantitated using the comparative method (ΔΔCT). Graphs represent the fold change of target gene expression in mutant compared to control samples. The Student's *t*-test was used for statistical analysis. $P < 0.05$ was considered to indicate a statistically significant difference.

2.5. Irradiation

Wild type or *eiger*^{1} mutant embryos at 8–9.5 h of age were irradiated with 4000 rads, and then recovered for 4 h at 25 °C. Following recovery, embryos were dechorionated and subjected to immunostaining, Western blotting and qRT-PCR.

3. Results and discussion

3.1. Eiger is expressed in the CNS glia and neurons during embryogenesis

We first characterized the *eiger* expression pattern by *in situ* hybridization during late embryogenesis, when massive neuronal apoptosis occurs [17,20]. As shown in Fig. 1, *eiger* transcripts are detected specifically in the embryonic CNS at these stages (Fig. 1A and B) similarly to the previously shown data in [21].

To follow Eiger protein expression, we stained wild type embryos with an anti-Eiger antibody (Fig. S1). Our staining displayed high levels of the Eiger protein on glial membranes labeled with GFP as well as in neurons (Fig. 1C–E). To bypass the possibility that Eiger can be cleaved and secreted, like its mammalian TNF-alpha counterpart [21,22], we monitored nuclear GFP (nucGFP) expression driven by *eigerGal4*, whose specificity was checked by immunostaining of *eigerGal4::UAScytGFP* embryos with the anti-Eiger antibody (Fig. S1C–C″). In *eigerG4::nucGFP* embryos, GFP was detected in certain neurons and glial cells using specific markers for neurons (anti-ELAV, Fig. 1G and H) and glia (anti-REPO, Fig. 1I and J), indicating that *eiger* is expressed in both cell types. Labeling specific subsets of neurons showed strong expression of nuclear GFP in CUT- and Tyrosine Hydroxylase (TH)-positive neurons with no or little expression in even-skipped (EVE)- or Dachshund (DAC)-positive neurons respectively (Fig. S2). These data reveal that Eiger is not equally expressed in all types of neurons, suggesting that it may have different functions in different neuronal subtypes.

3.2. Eiger is not required for developmental apoptosis in the CNS

The specific expression of Eiger in neurons and glia during late embryogenesis prompted us to test whether it is required for neuronal developmental apoptosis and/or glial phagocytic clearance of apoptotic cells occurring in the CNS at this stage. We first assessed apoptosis by labeling apoptotic cells with an anti-activated caspase 3 (CM1) antibody (Fig. 2A′, A″, B′, B″ and C). As Fig. 2C shows, the volume of apoptotic particles in the *eiger*^{1} mutant ventral nerve cord (VNC) is not significantly different than that of the wild type VNC (Fig. 2C), suggesting that lack of Eiger does not affect the overall levels of apoptosis in the CNS. However, since Eiger is expressed in neurons and glia, it could be involved in neuronal apoptosis and glial phagocytosis simultaneously, and therefore mutant phenotypes could mask each other. For example, reduced apoptosis might result in lower volume of apoptotic particles; however, impaired phagocytosis would cause apoptotic particles to persist for a longer time, resulting in a similar volume of apoptotic cells as in the wild type situation. To further evaluate whether developmental neuronal death was prevented in *eiger*^{1} mutant embryos, we counted different neuronal types (EVE, DAC and CUT) in *eiger*^{1} mutants, wild type embryos, and *H99* deficient embryos where apoptosis is prevented [23]. In the *H99* mutant embryonic neurons that normally die through apoptosis instead survive and their number is increased [20]. We expect that if in *eiger*^{1} mutants there is reduced neuronal apoptosis, different neuronal subtypes would survive and show higher number as compared to wild type

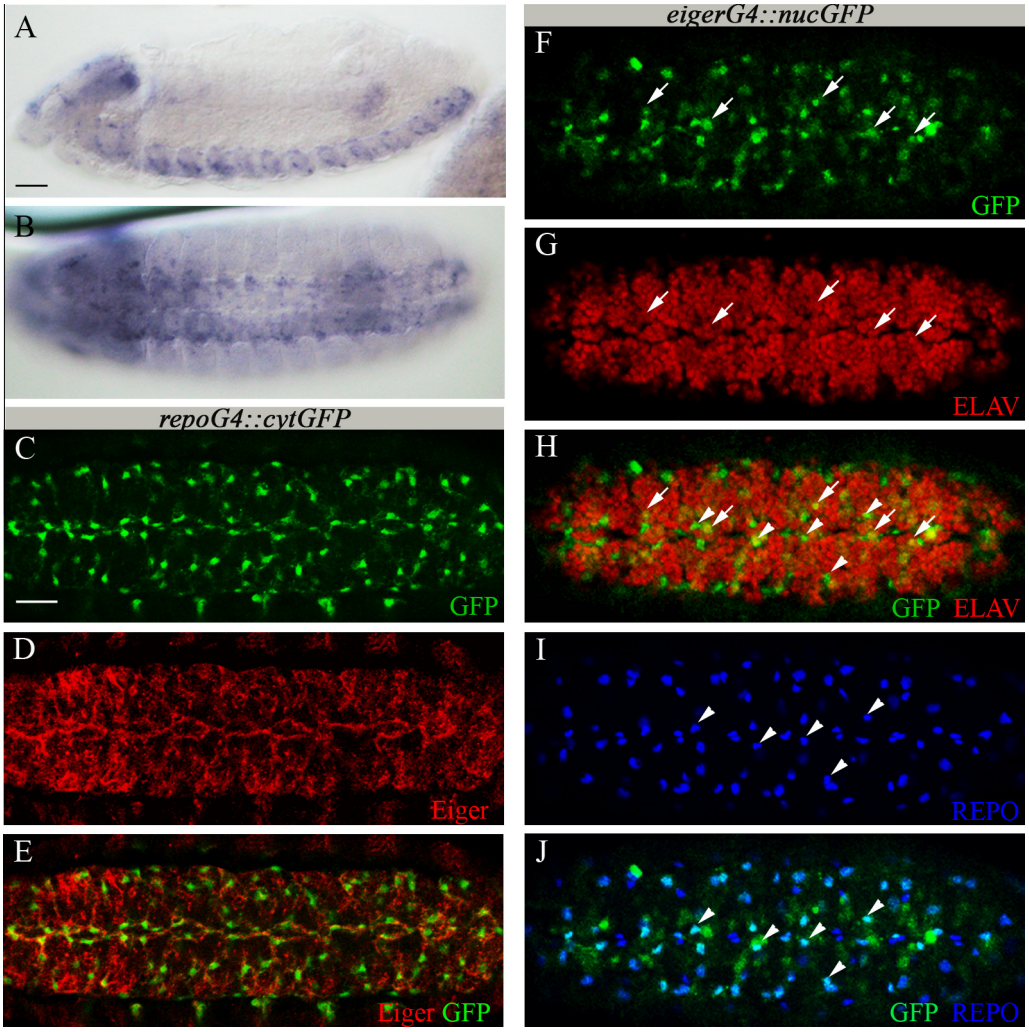

Fig. 1. Glia and specific neurons express Eiger. (A and B) RNA *in situ* hybridization (*eiger* ORF as probe) of whole mount embryos showing *eiger* transcript accumulation in the CNS. Lateral (A) and ventral (B) views. Bar, 20 μm. (C–J) Projections from confocal stacks of the CNS at embryonic stage 16, ventral view. Bar, 20 μm. (C–E) Embryo expressing cytoplasmic GFP under *repoGal4* driver (*repoGal4::cytGFP*) depicting glia in green (C) and anti-Eiger staining in red (D). (F–J) Embryos expressing nuclear GFP under *eigerGal4* driver (green) and stained with anti-ELAV (red) and anti-REPO (blue) antibodies. Some neurons expressing GFP are marked with arrows and some glial cells expressing GFP are marked with arrow heads.

embryos (Fig. 3J–L). However, no significant difference was obtained in the number of all three types of neurons between *eiger*^{1} and control embryos (Fig. 3J–L), indicating that lack of *eiger* does not prevent developmental neuronal death.

Next, we evaluated glial phagocytosis of apoptotic cells by labeling glial cells with an anti-SIMU antibody, which specifically recognizes the phagocytic transmembrane receptor Six Microns Under (SIMU) on glial membranes [18] (Fig. 2A, A″, B and B″) and therefore reveals whether an apoptotic particle is engulfed or unengulfed by a glial cell. We counted apoptotic particles untouched by glial cells and found the same percentage of untouched particles in *eiger*^{1} mutants and wild type embryos (Fig. 2D), indicating that engulfment of apoptotic particles proceeds normally in *eiger*^{1} mutants. Additionally, we monitored phagosomal activity of glia in live wild type and *eiger*^{1} mutant embryos using LysoTracker (LT), which specifically labels phagosomes and phagolysosomes (Fig. 2F–G″). In this case, glial cells were labeled using a *simu-cytGFP* construct, which comprises a *simu* promoter region fused to cytoplasmic GFP and is therefore expressed specifically in glia [17] (Fig. 2F, F″, G and G″). No significant difference in number of LT-positive particles between wild type and *eiger*^{1} mutant embryos was observed (Fig. 2E).

Thus, our comprehensive analysis of *eiger*^{1} mutant embryos demonstrates that *eiger* is not involved in developmental neuronal apoptosis or glial phagocytosis during late embryogenesis, despite its highly specific expression in the embryonic CNS at this stage, when massive neuronal apoptosis takes place and phagocytic glia efficiently clear apoptotic neurons.

3.3. Eiger overexpression does not promote apoptosis in the embryonic CNS

Ectopic expression of Eiger in the eye or wing imaginal discs leads to reduction of eye or wing size by inducing massive apoptosis [8,9]. However, we revealed that Eiger is not sufficient to induce apoptosis in embryonic neurons or glia in the CNS: when we overexpressed it in embryonic neurons or glia, using *elavGal4* or *repoGal4* drivers respectively (Fig. 3B–C″) we did not observe any difference in the volume of apoptotic particles (Fig. 3E) as compared to control embryos. Nor was there a significant difference in the numbers of EVE-, DAC- or CUT-positive neurons between embryos overexpressing *eiger* specifically in neurons and control embryos (Fig. 3H–H″ and J–L), indicating that Eiger overexpression in neurons does not lead to neuronal death. Similarly, no

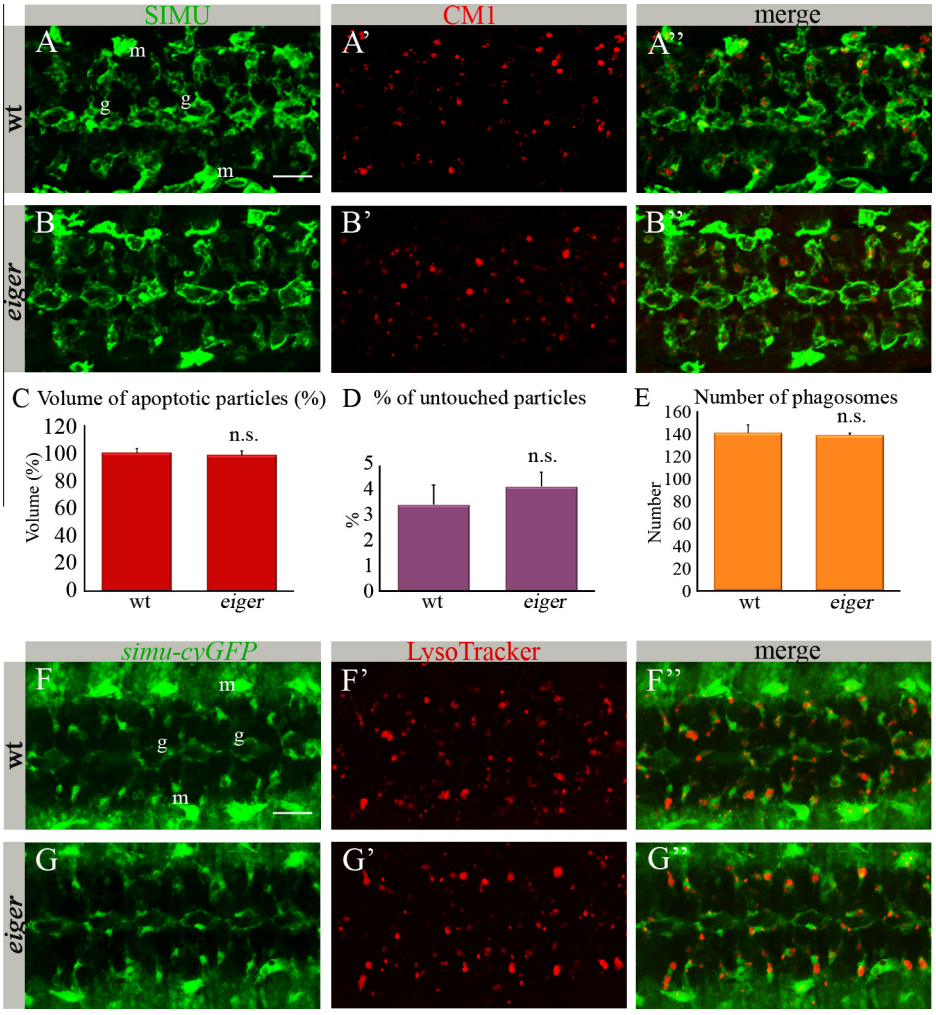

Fig. 2. Eiger is not required for developmental apoptosis in the embryonic CNS. (A–B″, F–G″) Projections from confocal stacks of the CNS at embryonic stage 16, ventral view. Bar, 20 μm. (A–B″) Apoptotic particles in red (CM1) and glia in green (anti-SIMU), g depicts glia, m depicts macrophages. (C) Columns represent mean total volume of apoptotic particles in 5 segments within confocal stacks (5 sections; total 7.5 μm) of the CNS, ±S.E.M., $n = 11–13$. There is no difference in *eiger*^{1} mutant compared to wild type embryos (100%). (D) Percentage of untouched apoptotic particles in wild type and *eiger*^{1} mutant embryos. Columns represent the ratio ± S.E.M., $n = 5–7$. (E) Number of phagolysosomes labeled with LT in wild type and *eiger*^{1} mutant embryos. Columns represent mean total number of LT-labeled phagolysosomes in 5 segments within 5 confocal stacks of the CNS, ±S.E.M., $n = 7$. (C–E) Data analyzed using Student's *t*-test. Error bars depict mean ± S.E.M.; n.s. (not significant) $P > 0.05$. (F–G″) Live imaging of *simu-cytGFP* labeled glia (g) and macrophages (m) following LT injections. (F–F″) Wild type and (G–G″) *eiger*^{1} mutant.

significant difference in the number of glial cells was detected between control embryos and embryos overexpressing *eiger* specifically in glia (Fig. S3), indicating that overexpression of Eiger in glia does not cause glial apoptosis.

Our data demonstrate that Eiger overexpression in embryonic neurons or glia is not sufficient to induce apoptosis in the developing CNS. This suggests that distinct molecular mechanisms control cell death of epithelial cells in imaginal discs, which are killed by Eiger through activation of the JNK pathway [8,9], and in the embryonic CNS where Eiger overexpression does not affect cell death. In order to determine whether Eiger activates the JNK pathway in embryogenesis we used a reporter, *TRE-eGFP*, that contains *Drosophila* AP-1 binding sites fused to the *eGFP* gene [24]. We detected comparable low expression levels of the *TRE-eGFP* reporter in the CNS of control and embryos overexpressing Eiger in neurons (Fig. S5 and data not shown), indicating that Eiger is unable to activate the JNK pathway in the embryonic CNS.

3.4. Eiger is required for HID-induced neuronal apoptosis

So far we found that, despite its specific expression in the embryonic CNS, *eiger* is not required for developmental apoptosis and that its overexpression is not sufficient to induce apoptosis during embryogenesis. It has been previously shown that transcription of *eiger* is highly induced by p53-mediated DNA damage following ionizing radiation (IR) of early embryos [25]. Therefore, we addressed the involvement of *eiger* in damage-induced cell death during CNS development. Since the embryonic CNS at stage 16 is no longer responsive to UV or IR [26], we mimicked damage-induced neuronal apoptosis by overexpressing the pro-apoptotic protein HID, which is a central player in damage-induced apoptosis following UV or IR [25,27,28]. In flies, *hid* is a target of p53, which is induced concomitantly with *eiger* following IR of early embryos. In the transgenic embryos specifically overexpressing HID in embryonic neurons *(elavGal4::hid)*, a significantly higher volume of apoptotic cells was detected as compared to control embryos (Figs. 2A' and 4D and H). In addition, a substantial reduction in the number of neuronal cell types CUT-, DAC- and EVE-positive was obtained as compared to their number in wild type embryos (Figs. 3I–L and 4A and G).

To test if Eiger is involved in *hid*-induced apoptosis, we overexpressed *hid* specifically in neurons of *eiger*^{1} mutant embryos using the *elavGa4* driver (*eiger*^{1}*;elavGal4::hid*) and measured the levels of CM1 staining. We found a significant decrease in the volume of

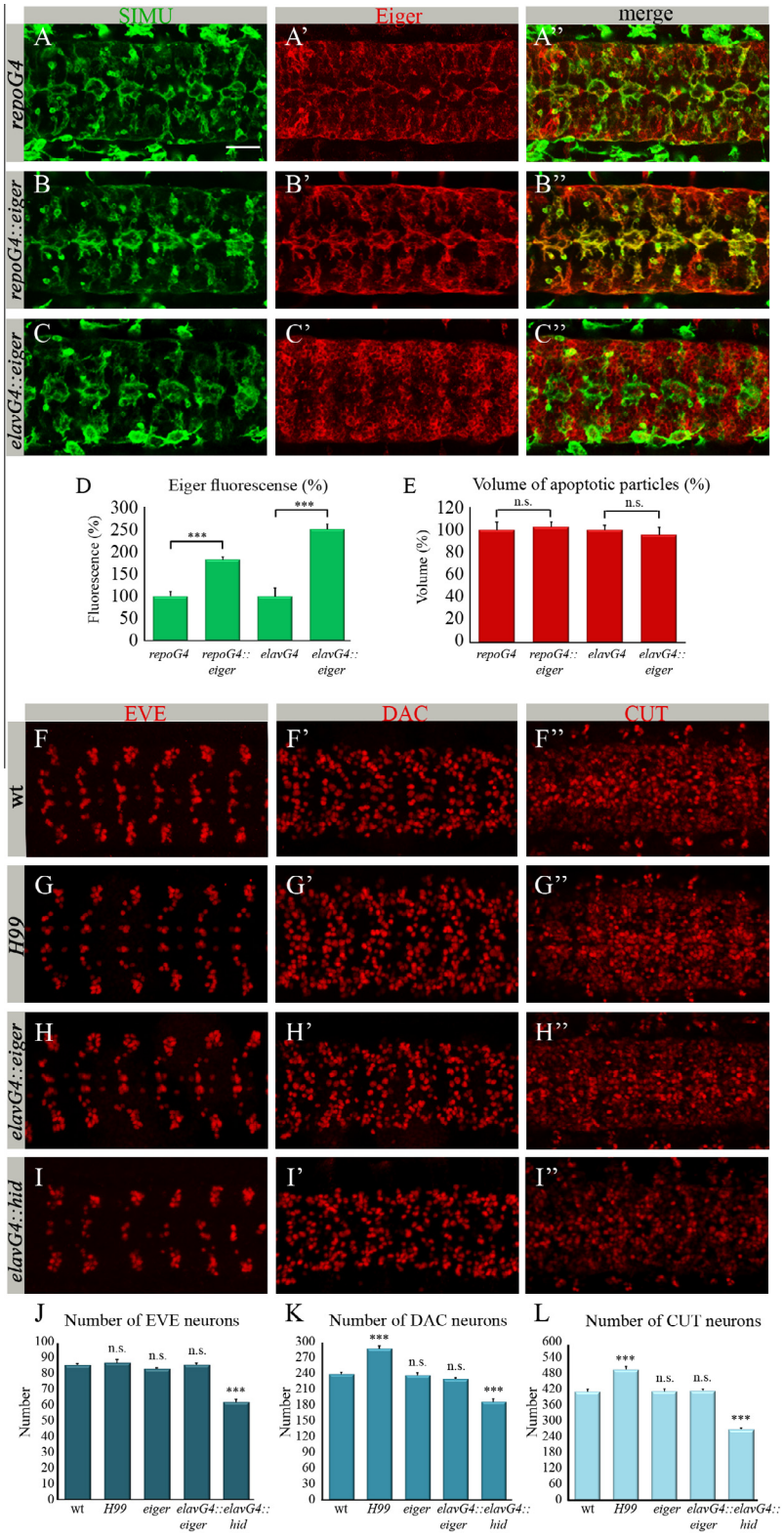

Fig. 3. Overexpression of Eiger in the embryonic CNS does not affect apoptosis. (A–C″, F–I″) Projections from confocal stacks of the CNS at embryonic stage 16, ventral view. Bar, 20 μm. (A–C″) Glia in green (anti-SIMU) and Eiger protein in red (anti-Eiger). (D) Relative fluorescence of anti-Eiger antibody as evaluation of Eiger overexpression. Columns represent relative total fluorescence of anti-Eiger antibody within 5 confocal stacks of the CNS, ±S.E.M., $n = 5–8$. (E) Columns represent mean total volume of apoptotic particles in 5 segments within 5 confocal stacks of the CNS, ±S.E.M., $n = 7–9$. There is no difference between *elavGal4* and *repoGal4* control embryos and *elavGal4::eiger* and *repoGal4::eiger* embryos. (F–I″) Staining with three different neuronal markers: anti-EVE, anti-DAC and anti-CUT, of wild type (F–F″), *H99* mutant (G–G″), *elavGa4::eiger* (H–H″) and *elavGa4::hid* (I–I″) embryos. (J–L) Quantification of different neuronal types. Columns represent mean total number of labeled neurons in 3 segments within confocal stacks of the CNS, ±S.E.M., $n = 5–10$. Note the increased number of DAC- and CUT-positive cells in H99 mutant embryos and no difference in number of EVE-positive cells. In *elavGa4::hid* embryos all neuronal types show a reduced number. To count the number of EVE and DAC neurons confocal stacks of the whole CNS (15 sections; total 22.5 μm) were acquired. To count the number of CUT-positive cells confocal stacks (4 sections; total 6 μm) were acquired from the neural cortex of stage 16 ventral nerve cords. (D, E, J–L) Asterisks indicate statistical significance versus control, as determined by Student's *t*-test, $^{***}P < 0.001$, n.s. (not significant) $P > 0.05$.

CM1-positive particles in these embryos as compared to *elavGal4::hid* control embryos whereas the overall CNS appeared close to normal (Fig. 4E, E″ and H), indicating a substantial suppression of the *hid* overexpression phenotype by lack of *eiger*. In addition, to determine whether the reduction in apoptosis rate assessed by cleaved caspase 3 levels results in neuronal survival, we counted specific neuronal cell types in *eiger*^{1} mutant embryos overexpressing *hid* in neurons and compared their number to wild type and control embryos. A significantly higher number of DAC- and CUT-positive neurons was detected in mutants as compared to control embryos (Fig. 4B and G, S4), indicating that a greater proportion of *hid*-expressing neurons survive in the absence of *eiger*. Importantly, DAC-positive neurons normally do not express Eiger whereas CUT-positive neurons do (Fig. S2), suggesting that Eiger may affect neuronal death non-autonomously. This effect is possibly mediated by Eiger itself, which can be cleaved and released from the cell surface as a soluble factor [21,29]. In any case, our data propose that Eiger is required for HID-induced neuronal death in the embryonic CNS.

3.5. Eiger is required for maintaining HID levels independently of dJNK signaling

To understand how Eiger influences HID-induced neuronal death we examined levels of the HID protein in control and *eiger*^{1} mutant embryos overexpressing *hid* specifically in neurons (*elavGal4::hid* and *eiger*^{1}*;elavGal4::hid* respectively). By Western blot analysis of embryonic lysates (Fig. 4J) using an anti-HID

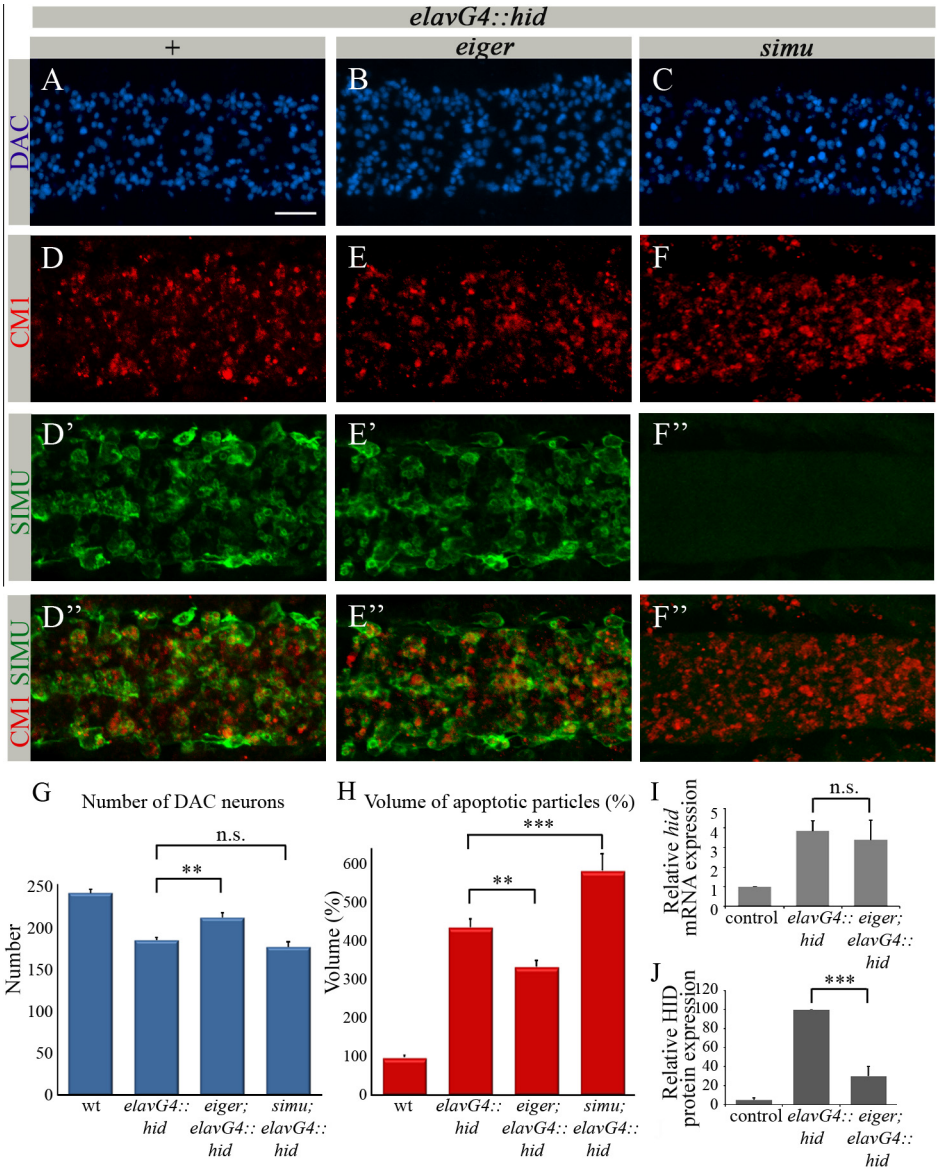

Fig. 4. Eiger is required for *hid*-induced neuronal apoptosis. (A–F″) Projections from confocal stacks of the CNS at embryonic stage 16, ventral view. Bar, 20 μm. (A–C) DAC-positive neurons (blue) in *elavGal4::hid*, *eiger*^{1}*;elavGal4::hid* and *simu;elavGal4::hid* embryos. (D–F″) Apoptotic particles in red (CM1) and glia in green (anti-SIMU) in the same embryos as in (A–C). (G) Quantification of DAC-positive neurons as described in Fig. 3. Columns represent mean total number of labeled neurons within confocal stacks of the CNS, ±S.E.M., n = 10–15. (H) Columns represent mean total volume of apoptotic particles in 5 segments within 5 confocal stacks of the CNS, ±S.E.M., n = 7–10. (G, H) Asterisks indicate statistical significance versus control, as determined by Student's t-test, $^{**}P < 0.008$, n.s. (not significant) $P > 0.05$. (I) qRT-PCR for *hid* on wild type, *elavGal4::hid* and *eiger*^{1}*;elavGal4::hid* embryos; bars represent mean ± S.E.M. No significant changes (n.s. $P > 0.05$) in levels of *hid* expression are detected based on Student's t-test analysis. (J) Quantification using TotalLab Quant software of HID protein levels detected by Western blot analysis of 100 μg protein from embryonic lysates of wild type, *elavGal4::hid* and *eiger*^{1}*;elavGal4::hid* embryos using anti-HID and anti-Actin antibodies. Columns represent mean band volume normalized to *elavGal4::hid*. Asterisks indicate statistical significance versus *elavGal4::hid*, as determined by Student's t-test, $^{***}P < 0.001$.

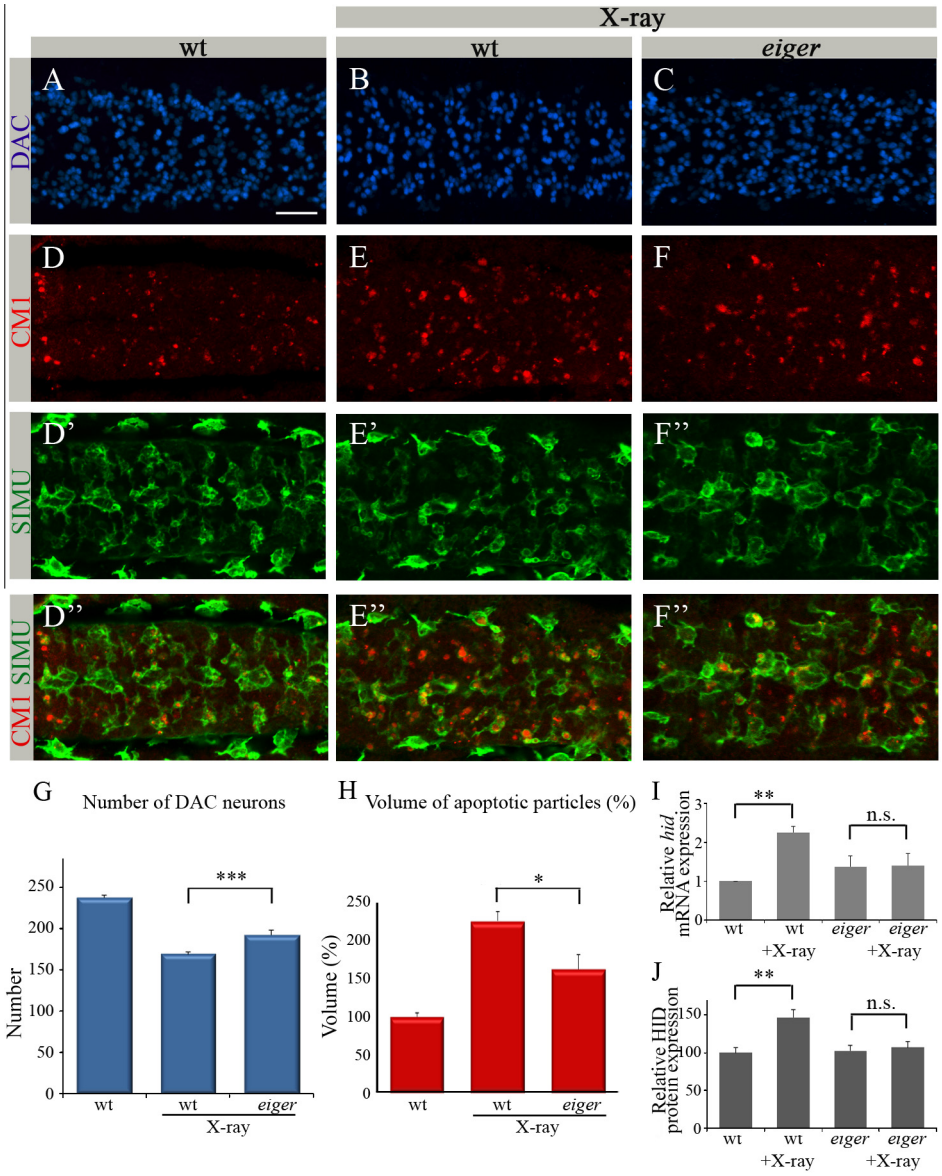

Fig. 5. Eiger is required for X-ray induced apoptosis in young embryos. (A–F″) Projections from confocal stacks of the CNS at embryonic stage 16, ventral view. Bar, 20 μm. (A–C) DAC-positive neurons (blue) in wild type without irradiation, wild type and *eiger*^{1} embryos following irradiation. (D-F″) Apoptotic particles in red (CM1) and glia in green (anti-SIMU) in wild type without irradiation, wild type and *eiger*^{1} embryos following irradiation. (G) Quantification of DAC-positive neurons as described in Fig. 3. Columns represent mean total number of labeled neurons within confocal stacks of the CNS, ±S.E.M., $n = 10–12$. (H) Columns represent mean total volume of apoptotic particles in 5 segments within 5 confocal stacks of the CNS, ±S.E.M., $n = 5–6$. (G, H) Asterisks indicate statistical significance versus control, as determined by Student's *t*-test, $^{***}P < 0.0007$, $^{*}P < 0.02$. (I) qRT-PCR for *hid* on wild type and *eiger*^{1} mutants before and following X-ray irradiation; bars represent mean ± S.E.M. Asterisks indicate statistical significance versus non-irradiated control, as determined by Student's *t*-test, $^{**}P < 0.005$. No significant changes (n.s. $P > 0.05$) in levels of *hid* expression are detected based on Student's *t*-test analysis. (J) Quantification using TotalLab Quant software of HID protein levels detected by Western blot analysis of 100 μg protein from embryonic lysates of wild type, and *eiger*^{1} mutant embryos using anti-HID and anti-Actin antibodies before and after irradiation. Columns represent mean band volume normalized to wild type. Asterisks indicate statistical significance versus control, as determined by Student's *t*-test, $^{**}P < 0.005$.

antibody we detected a significant reduction in levels of HID in *eiger*^{1} mutant embryos as compared to control embryos, suggesting that lack of Eiger affects HID protein levels (Fig. 4J). To explore whether *eiger* affects *hid* transcription we performed quantitative RT-PCR (qRT-PCR) analysis of *hid* mRNA in control (*elavGal4::hid*) and *eiger*^{1} mutant embryos (*eiger*^{1}*; elavGal4::hid*). Our data demonstrate the same levels of *hid* transcripts in the control and *eiger*^{1} mutants (Fig. 4I) suggesting that *eiger* is required for expression or stabilization of the HID protein and not for its transcriptional regulation in this system.

In addition, to test whether *eiger*-mediated effect on apoptosis is specific for *hid* expression we tested overexpression of the pro-apoptotic gene *reaper* in embryonic neurons using the *elavGal4* driver. No significant difference was observed in level of apoptosis between wild type and *eiger*^{1} embryos (Fig. S6), suggesting that *eiger* influences damage-induced apoptosis specifically through *hid*.

Eiger has been previously shown to induce apoptosis as a ligand of the JNK signaling pathway [8,9,21]. Therefore, we tested activation of the JNK pathway in *elavGa4::hid* embryos using the *TRE-eGFP* reporter. We detected comparable low expression levels of GFP in the CNS of control and *elavGal4::hid* embryos, indicating that neuronal-specific expression of HID and induction of apoptosis do not activate the JNK pathway in the embryonic CNS (Fig. S5). These data suggest that Eiger affects HID-induced apoptosis independently of JNK signaling.

3.6. Eiger plays a role in X-ray-induced apoptosis

To further understand Eiger's function in damage-induced apoptosis and its effect on HID function we irradiated young wild type and *eiger*^{1} mutant embryos at stage 12–13 (8–9.5 h). Embryos at this stage are still sensitive to IR [26] and already express *eiger* [21]. Following irradiation and recovery of 4 h, we examined the levels of apoptosis by evaluating the volume of CM1-positive particles (Fig. 5D–F″ and H) as well as by counting DAC neurons (Fig. 5A–C and G). These results revealed significantly lower level of apoptosis in *eiger*^{1} mutant embryos as compared to wild type embryos (Fig. 5H and G). In addition, to explore whether the obtained difference in apoptosis is a result of HID function, we assessed expression levels of *hid* mRNA by qRT-PCR (Fig. 5I) and HID protein levels by Western blot analysis (Fig. 5J) in wild type and *eiger*^{1} mutant embryos subjected to IR.

Following IR, significantly lower *hid* mRNA and protein expression was detected in *eiger*^{1} mutants as compared to wild type embryos, suggesting that *eiger* is required for the increase in *hid* levels following X-ray exposure. These data place *eiger* function upstream to *hid* in damage-induced apoptosis and suggest a role for *eiger* in regulation of *hid* expression following damage. Lower HID protein levels in *eiger*^{1} mutants likely result from reduced transcription as detected by qRT-PCR, but translational or post-translational regulation of *hid* cannot be ruled out.

It has been previously shown that ectopic *eiger* expression in eye imaginal discs induces *hid* mRNA expression [9] and that *eiger* is required for *hid* expression in pole cells [11]. Our study reveals that following neuronal damage during embryogenesis *eiger* plays a critical role in controlling *hid* at the transcriptional and translational levels.

3.7. Impaired phagocytosis of apoptotic cells does not prevent death of damaged neurons

Since Eiger is expressed in the embryonic phagocytic glia, we were interested to determine whether compromised glial phagocytosis could also be involved in survival of damaged neurons in *eiger*^{1} mutant embryos (*eiger*^{1}*;elavGal4::hid*) as compared to control (*elavGal4::hid*) embryos. Given that reduced apoptosis was detected in *eiger*^{1}*;elavGal4::hid* embryos, possible defects in phagocytosis might be masked. Therefore, in order to understand whether survival of dying neurons in the mutant embryos may result from their impaired engulfment, we examined neuronal survival in embryos with compromised phagocytosis. SIMU is a glial phagocytic receptor, which is required for recognition and engulfment of apoptotic particles [17]. *simu* mutant embryos are strongly impaired in their ability to recognize and engulf apoptotic cells and exhibit a high number of unengulfed apoptotic neurons in the embryonic CNS [17]. When we tested *simu* mutant embryos expressing *hid* in neurons (*simu; elavGal4::hid*), we detected a higher volume of apoptotic particles in their CNS as compared to control *elavGal4::hid* embryos (Fig. 4D, F and H). However, when we counted DAC-positive neurons in *simu* mutants overexpressing *hid* in neurons we could not find any increase in their number as compared to control embryos (Fig. 4A, C and G) suggesting that compromised phagocytosis did not prevent death of DAC-positive damaged neurons. Based on these results we propose that in *eiger*^{1} mutants glial phagocytosis does not play a role in preventing the execution of damaged neurons, which is in contrast to the previously described role of phagocytic genes in execution of developmental apoptosis in *Caenorhabditis elegans* [30,31].

In this study, we reveal a novel role for *Drosophila* TNF-alpha in elimination of damaged neurons during development by controlling levels of the pro-apoptotic gene *hid*, which is crucial for the life-or-death decision that a damaged cell has to make. This finding opens new directions for exploring *eiger* function in the developing and mature nervous system.

Conflict of interest

All authors declare no conflict of interest.

Acknowledgments

We would like to thank B. Jones, D. Bohmann, G.W. Davis, E. Arama, H. Steller, M. Miura, O. Schuldiner, A. Salzberg, Hybridoma bank and the Bloomington Stock Center for generously providing fly strains and antibodies. We thank Dr. Alexander Nevelsky and Egor Borzov from Department of Oncology, Rambam Medical Center (RMC) for their assistance in the X-ray experiments. We thank Z. Paroush and T. Schultheiss for comments on the manuscript and the Kurant laboratory members for constructive criticism and support. We also thank E. Suss-Toby at the Interdepartmental Bioimaging facility for excellent technical support. We gratefully acknowledge financial support from Rappaport Institute and from Allen and Jewell Prince Center for Neurodegenerative Disorders of the Brain.

Appendix A. Supplementary data

Supplementary data associated with this article can be found, in the online version, at http://dx.doi.org/10.1016/j.febslet.2015.02.032.

References

[1] Locksley, R.M., Killeen, N. and Lenardo, M.J. (2001) The TNF and TNF receptor superfamilies: integrating mammalian biology. Cell 104 (4), 487–501.
[2] Aggarwal, B.B. (2003) Signalling pathways of the TNF superfamily: a double-edged sword. Nat. Rev. Immunol. 3 (9), 745–756.
[3] Wajant, H., Pfizenmaier, K. and Scheurich, P. (2003) Tumor necrosis factor signaling. Cell Death Differ. 10 (1), 45–65.
[4] Vujanovic, N.L. (2011) Role of TNF superfamily ligands in innate immunity. Immunol. Res. 50 (2–3), 159–174.
[5] Maecker, H. et al. (2005) TWEAK attenuates the transition from innate to adaptive immunity. Cell 123 (5), 931–944.
[6] Liu, J. and Lin, A. (2005) Role of JNK activation in apoptosis: a double-edged sword. Cell Res. 15 (1), 36–42.
[7] Balkwill, F. (2009) Tumour necrosis factor and cancer. Nat. Rev. Cancer 9 (5), 361–371.
[8] Igaki, T. et al. (2002) Eiger, a TNF superfamily ligand that triggers the Drosophila JNK pathway. EMBO J. 21 (12), 3009–3018.
[9] Moreno, E., Yan, M. and Basler, K. (2002) Evolution of TNF signaling mechanisms: JNK-dependent apoptosis triggered by Eiger, the Drosophila homolog of the TNF superfamily. Curr. Biol. 12 (14), 1263–1268.
[10] Schneider, D.S. et al. (2007) Drosophila eiger mutants are sensitive to extracellular pathogens. PLoS Pathog. 3 (3), e41.
[11] Maezawa, T. et al. (2009) Expression of the apoptosis inducer gene head involution defective in primordial germ cells of the Drosophila embryo requires eiger, p53, and loki function. Dev. Growth Differ. 51 (4), 453–461.
[12] Bidla, G., Dushay, M.S. and Theopold, U. (2007) Crystal cell rupture after injury in Drosophila requires the JNK pathway, small GTPases and the TNF homolog Eiger. J. Cell Sci. 120 (Pt. 7), 1209–1215.
[13] Wang, H. et al. (2006) Drosophila homologs of mammalian TNF/TNFR-related molecules regulate segregation of Miranda/Prospero in neuroblasts. EMBO J. 25 (24), 5783–5793.
[14] Kato, K., Awasaki, T. and Ito, K. (2009) Neuronal programmed cell death induces glial cell division in the adult Drosophila brain. Development 136 (1), 51–59.
[15] Igaki, T. et al. (2009) Intrinsic tumor suppression and epithelial maintenance by endocytic activation of Eiger/TNF signaling in Drosophila. Dev. Cell 16 (3), 458–465.
[16] Cordero, J.B. et al. (2010) Oncogenic Ras diverts a host TNF tumor suppressor activity into tumor promoter. Dev. Cell 18 (6), 999–1011.
[17] Kurant, E. et al. (2008) Six-microns-under acts upstream of Draper in the glial phagocytosis of apoptotic neurons. Cell 133 (3), 498–509.
[18] Shklyar, B. et al. (2013) Caspase activity is required for engulfment of apoptotic cells. Mol. Cell. Biol. 33 (16), 3191–3201.
[19] Shklyar, B., Shklover, J. and Kurant, E. (2013) Live imaging of apoptotic cell clearance during Drosophila embryogenesis. J. Vis. Exp., 78.

[20] Rogulja-Ortmann, A. et al. (2007) Programmed cell death in the embryonic central nervous system of Drosophila melanogaster. Development 134 (1), 105–116.
[21] Kauppila, S. et al. (2003) Eiger and its receptor, Wengen, comprise a TNF-like system in Drosophila. Oncogene 22 (31), 4860–4867.
[22] Narasimamurthy, R. et al. (2009) Structure-function analysis of Eiger, the Drosophila TNF homolog. Cell Res. 19 (3), 392–394.
[23] White, K. et al. (1994) Genetic control of programmed cell death in Drosophila. Science 264 (5159), 677–683.
[24] Chatterjee, N. and Bohmann, D. (2012) A versatile PhiC31 based reporter system for measuring AP-1 and Nrf2 signaling in Drosophila and in tissue culture. PLoS ONE 7 (4), e34063.
[25] Brodsky, M.H. et al. (2004) Drosophila melanogaster MNK/Chk2 and p53 regulate multiple DNA repair and apoptotic pathways following DNA damage. Mol. Cell. Biol. 24 (3), 1219–1231.
[26] Zhou, L. and Steller, H. (2003) Distinct pathways mediate UV-induced apoptosis in Drosophila embryos. Dev. Cell 4 (4), 599–605.
[27] Bilak, A. and Su, T.T. (2009) Regulation of Drosophila melanogaster pro-apoptotic gene hid. Apoptosis 14 (8), 943–949.
[28] Jassim, O.W., Fink, J.L. and Cagan, R.L. (2003) Dmp53 protects the Drosophila retina during a developmentally regulated DNA damage response. EMBO J. 22 (20), 5622–5632.
[29] Pérez-Garijo, A., Fuchs, Y. and Steller, H. (2013) Apoptotic cells can induce non-autonomous apoptosis through the TNF pathway. eLife 2, e01004.
[30] Hoeppner, D.J., Hengartner, M.O. and Schnabel, R. (2001) Engulfment genes cooperate with ced-3 to promote cell death in *Caenorhabditis elegans*. Nature 412 (6843), 202–206.
[31] Reddien, P.W., Cameron, S. and Horvitz, H.R. (2001) Phagocytosis promotes programmed cell death in *C. elegans*. Nature 412 (6843), 198–202.